Measurement of Rotor Thermal Time-Constant for Permanent Magnet Synchronous Machines

Eric Armando
Dipartimento Energia "G.Ferraris"
Politecnico di Torino
Torino, Italy
eric.armando@polito.it

Aldo Boglietti
Dipartimento Energia "G.Ferraris"
Politecnico di Torino
Torino, Italy
aldo.boglietti@polito.it

Salvatore Musumeci
Dipartimento Energia "G.Ferraris"
Politecnico di Torino
Torino, Italy
salvatore.musumeci@polito.it

Sandro Rubino
Dipartimento Energia "G.Ferraris"
Politecnico di Torino
Torino, Italy
sandro.rubino@polito.it

Enrico Carpaneto
Dipartimento Energia "G.Ferraris"
Politecnico di Torino
Torino, Italy
enrico.carpaneto@polito.it

Daniele Martinello
Dipartimento Energia "G.Ferraris"
Politecnico di Torino
Torino, Italy
daniele.martinello@polito.it

***Abstract*—Thanks to their high torque density, permanent magnet synchronous motors (PMSMs) currently represent the most competitive solution in the electrification processes involving transports and energy production. However, it is known how the torque production of such motors is strictly related to the temperature of the permanent magnet (PM), affecting control performance, and efficiency. This issue makes necessary the thermal analysis of the machine, thus requiring the determination of the PM's thermal time-constant. In this paper, an experimental method for evaluating such a parameter is proposed, allowing high accuracy and reliability of the result. The proposed procedure can be applied to any PMSM type, without being affected by factors such as rotor lamination, shaft, PM distribution. The experimental validation has been carried out on three PMSMs, having different rotor structure, sizes, and voltage/current levels. Experimental results demonstrate the validity of the proposed method.**

Keywords—permanent magnet synchronous motors, thermal analysis, thermal time-constant, transportation electrification.

I. Introduction

In recent years, significant development has concerned the electric solutions for transports and energy production from renewable [1]. Modern applications like electric and hybrid vehicles [2], [3], more electric aircraft, and railway traction require electric motors having a high torque density together with a strong overload capability. Therefore, following the needs of the market, the conventional induction machines (IMs) have been progressively replaced with the more performant permanent magnet synchronous motors (PMSMs), increasing efficiency and reducing weight and volume [4].

However, compared to the IMs, the torque production of the PMSMs is significantly affected by the temperature of the permanent magnet (PM), whose effect is to reduce the PM flux density [5]. Consequently, the torque production is compromised [6], thus making it necessary to increase the current injected in the machine to compensate for the PM flux drop. However, this action reduces the PMSM efficiency and leads to higher Joule losses with consequent thermal stress. Besides, the presented issue gets worse in the case of machine overload, thus requiring accurate thermal modeling [7], [8].

The thermal model of the PMSM allows for understanding several aspects, such as the evaluation of the limits in terms of injected stator currents, avoiding an excessive overheating of the PM. Indeed, the magnetic proprieties of the PM are thermal-sensitive under two aspects [5]. The first is related to the before-mentioned reduction of the PM flux density, although such effect is reversible. Indeed, in the case of PM cooling, the initial magnetic properties are restored fully. Conversely, the second aspect is related to the non-reversible PM demagnetization that can be caused by excessive PM heating. Both aspects get worse in the case of PMSM using fractional-slot windings, thus characterized by a high harmonic content on the magneto-motive force of the air gap [9]. In this case, the harmonic fields induce parasitic currents on the PM surface, increasing losses and PM temperature.

Therefore, for implementing proper overload control strategies, most of the modern electric drives for PMSMs often use two kinds of thermal feedback. The first is related to the temperature measurements provided by the thermal sensors embedded with the machine (e.g., thermocouples). The second feedback is provided by the machine thermal model [7] that is implemented in parallel with the motor control algorithm. However, both feedbacks are often related to the measured/estimated temperature of the stator winding, representing the most critical part of the machine. Therefore, the thermal sensors are usually placed on the stator winding surface, thus neglecting the thermal effects on the rotor. Concerning the thermal models of the machine, they usually consist of first- or second-order equation systems that are focused on the evaluation of the average temperature of the stator winding [10], [11].

Based on the literature, several attempts have been made to evaluate the PM temperature, proposing both direct and indirect methods [12]–[14]. The direct techniques are based on the evaluation of the PM-induced back-emf [14], directly related to the PM flux density, and thus proportional to the PM temperature. The indirect methods are based on the implementation of a proper thermal model [12], [13], considering all the machine design data (e.g., materials' proprieties, geometric dimensions of both PM and air gap). Both methods present advantages and disadvantages. The direct methods are not affected by design factors such as rotor lamination and PM distribution. However, they require the on-line measurement of the PM-induced back-emf. Conversely, the on-line implementation of the thermal models requires as inputs the estimation of the Joule- and iron losses, i.e., the conventional measurements of stator currents and mechanical speed (electrical frequency). However, all machine design data must be known.

The goal of this paper is to combine the advantages of mentioned-above methods by evaluating the PM's thermal time-constant experimentally. In detail, the proposed procedure is based on the measurements of the PM-induced back-emf, avoiding the needing for other motor losses [15], [16], that hinder the evaluation of PM's thermal parameters

with high accuracy. Therefore, the main advantage of the proposed method consists of getting the value of the PM thermal-time constant with a low level of uncertainty. In this way, the obtained value could be used as a starting point for the implementation of a robust and accurate thermal model of the PM. In summary, compared to the existing literature, the contributions of the proposed procedure are:

1) accurate evaluation of the PM's thermal-time constant of any PMSM, regardless of the PM distribution;
2) real-time monitoring of the stator winding temperature and PM flux-density during the thermal transients, allowing the correlation between them.

The experimental validation of the proposed measurement technique has been carried out on three low-power PMSMs that present a different PM distribution on the rotor. This paper builds on [17] and brings in added value by including:

- experimental validation on a new PMSM having a surface-mount PM distribution;
- evaluation of the derating that affects the torque production of the PMSMs after the PM heating;
- further considerations related to the impact of the PM heating on the machine efficiency.

The paper is organized as follows. The description of the proposed measurement technique is reported in Section II. The computation method of the PM's thermal time-constant is described in Section III. Experimental validation is provided in Section IV. Final remarks are reported in Section V while the conclusions are reported in Section VI.

II. Measurement Technique

The test bench for evaluating the PM's thermal time-constant is shown in Fig. 1, corresponding to the experimental setup used for the identification of the magnetic model of synchronous ac motors [18]–[20]. The motor under test (MUT) is connected to a driving machine (DM) that imposes the speed. Two possible configurations can be adopted. The first one consists of a back-to-back configuration (Fig. 1 - top) where the voltage source inverters (VSIs) of both MUT and DM share the same dc bus, i.e., dc-link voltage v_{dc}. Alternatively, a dedicated test rig for the DM (Fig. 1 - bottom) can be used.

A. Experimental test rig

According to the test bench used for the experimental validation, the second configuration is considered, whose layout is shown in Fig. 2. Compared to Fig. 1 and Fig. 2, showing the test rig for the identification of the flux linkage maps of the MUT, the presence of a torque sensor along the mechanical connection between MUT and DM is not necessary for the proposed test procedure. The DM can consist of an industrial spindle drive, whose electric machine is speed-controlled. Conversely, the MUT is current-controlled using a field-oriented control (FOC) scheme implemented in (dq) coordinates [21]. The rotor position of MUT is measured using a mechanical sensor (e.g., resolver or encoder).

The proposed test procedure requires the measurements of phase-voltages, phase-currents, and mechanical rotor position (Fig. 2). The measurements of phase-currents, together with that of the dc-link voltage, are also necessary to perform the FOC algorithm. The latter is implemented on a digital controller providing the duty-cycles commands to the VSI feeding the MUT.

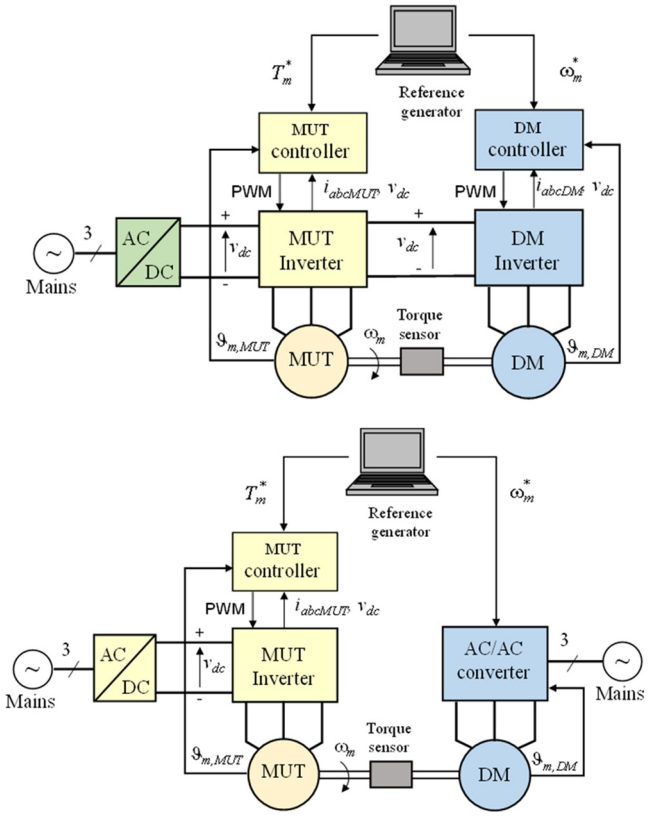

Fig. 1. Test rig for the PM thermal time constant determination: back-to-back configuration (top), dedicated test rig for DM (bottom).

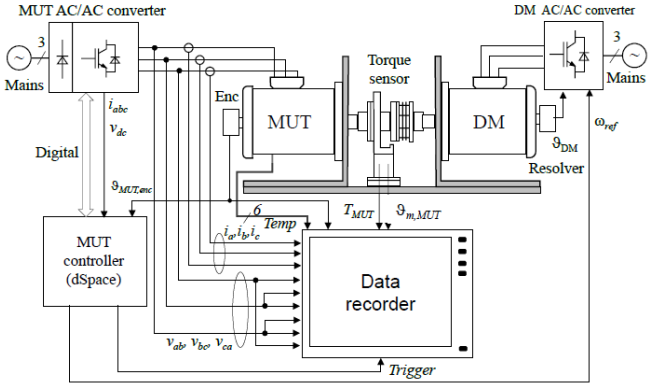

Fig. 2. Layout of the experimental test rig [20].

The measurement of the phase-voltages using a data recorder is proposed [19], without requiring the estimation of VSI voltage errors [22]. Therefore, the line-to-line voltages of the MUT are directly measured using high-voltage/high-speed acquisition channels [20]. However, since the pulse-width modulation (PWM) voltage signals are sampled, the reconstruction of the time-fundamental components must be performed. This action can be achieved by elaborating sampled data with the software integrated with the instrument. Besides, if a data recorder is employed, the measurements of mechanical rotor position, phase-currents, and line-to-line voltages are stored on the instrument, as shown in Fig. 2.

Finally, the DM usually consists of a standard spindle drive that is speed-controlled, and whose reference is provided by the digital controller, as shown in Fig. 2. It is highlighted how the rated power of the DM can be very low, as the proposed procedure does not require the torque production of the MUT.

B. *Test procedure*

The proposed test procedure performs the heating of the MUT to monitor the increment of the stator winding resistance R_s and the decay of the PM flux linkage λ_m. The first is related to the average temperature of the stator winding T_s, while the decay of the PM flux linkage is representative of the PM's average temperature. After performing the heating procedure, the temperature of the stator winding should be equal to the rated one. Therefore, the time duration of the heating procedure can be a few minutes up to several hours, according to the machine dimensions, i.e., its thermal time-constant.

During the heating procedure, the time evolutions of the stator winding resistance and PM flux linkage should be acquired with a proper time-resolution Δt. According to the usual time-duration of the thermal transients involving the electrical machines [7], [23], a good compromise consists of evaluating both variables with a time-resolution of 1-3 minutes. Consequently, the heating procedure consists of a sequence of a predefined number n of thermal points. In each thermal point, three actions are performed: MUT heating, identification of the stator resistance followed by that of the PM flux linkage.

An application example is presented, facilitating understanding. A machine having an overall thermal time-constant of 60 minutes is considered. Therefore, for reaching the steady-state thermal conditions, the time-duration of the heating procedure should be at least five times the value of the thermal time-constant, corresponding to 300 minutes. As a consequence, assuming that time evolutions of the stator winding resistance and PM flux linkage must have a time-resolution of 3 minutes (Δt), the resulting number of thermal points composing the heating procedure is n = 100 (300/3).

In each thermal point, the heating action is performed by injecting a predefined combination of (dq) currents in the MUT, using a standard FOC scheme [21]. The amplitude of the current vector $I_{th,pk}$ should be set for injecting the RMS thermal current $I_{th,rms}$ of the MUT ($I_{th,pk} = \sqrt{2} \cdot I_{th,rms}$). Therefore, such a value usually corresponds to the rated current of the machine. Although there are no constraints on the distribution of the thermal current amplitude on the (dq) axes, the q-axis current component is set at zero. In this way, the torque production of the MUT is avoided. Therefore, the proposed test procedure consists of controlling actively only the d-axis current component, leading to the profile shown in Fig. 3. It is noted how, after the MUT heating, the identification of both stator resistance and PM flux linkage in each thermal point is performed.

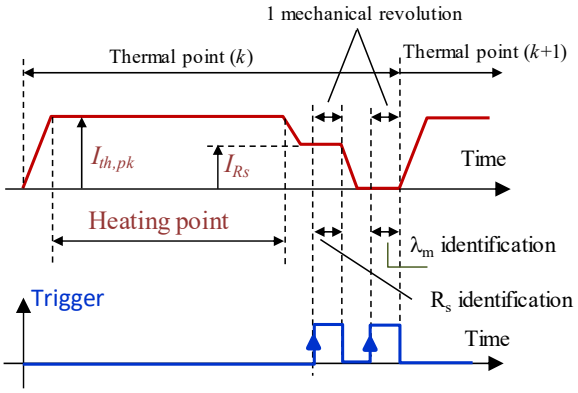

Fig. 3. Profile of the d-axis current in a generic thermal point k [19].

Concerning the identification of the stator resistance, the d-axis current component is set at a predefined target I_{Rs}. Such a value should guarantee the proper identification of the stator resistance, avoiding excessive MUT heating. Therefore, it is recommended to set the value of the current reference I_{Rs} lower than the thermal current, as shown in Fig. 3.

Each thermal point ends with the identification of the PM flux linkage. This variable is estimated by sensing the PM-induced back-emf, thus requiring to control both (dq) current components at zero (Fig. 3). The MUT speed must be kept constant as much as possible through the DM, and its value must allow proper back-emf sensing. Besides, the value of the MUT speed must be chosen to avoid significant losses on the iron of the MUT stator.

Finally, at the procedure end, all measurements collected by the data recorder are elaborated to get the PM's thermal time-constant. The flow diagram summarizing the proposed test procedure is shown in Fig. 4.

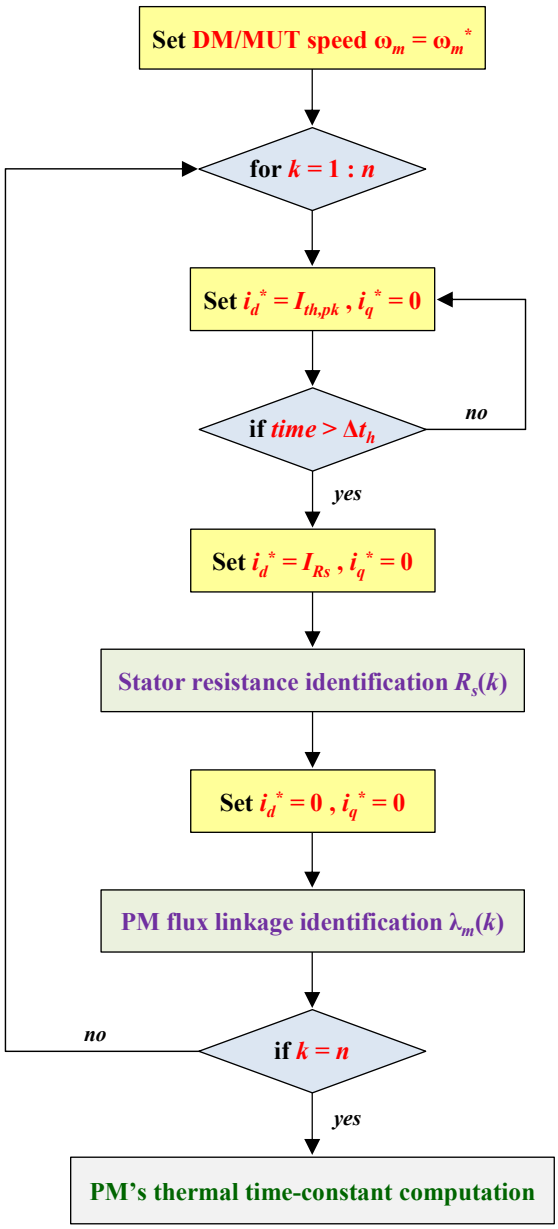

Fig. 4. Flow diagram of the proposed test procedure.

C. Identification of stator resistance and PM flux linkage

For each thermal point, the measurements of phase-currents, line-to-line voltages, and mechanical rotor position are performed. The latter, according to the number of pole pairs p of the MUT, is used to compute the d-axis position. Regarding the mounting offset of the mechanical sensor (e.g., resolver or encoder), this is compensated using the conventional commissioning procedures of the electric drives. Once the d-axis position is known, the Park transformation on the sampled values of phase-currents and line-to-line voltages is applied [21]. In this way, the (dq) components of stator currents (i_d,i_q) and stator voltages (v_d,v_q) are computed. It is highlighted how (dq) voltages are computed from the time-fundamental components of the line-to-line voltages. These are obtained by processing the voltage measurements with the software integrated with the data recorder [20].

1) Identification of the stator winding resistance and average stator winding temperature

The generic thermal point k (k = 1,…,n) is considered. The d-axis components of voltage and currents are computed as the average of all measurements performed in one mechanical revolution, thus mitigating the effects of the stator slots. Therefore, the stator resistance at the generic thermal point k (k = 1,…,n) is computed as:

$$R_s(k) = \frac{V_d(k)}{I_d(k)} \cong \frac{V_d(k)}{I_{R_s}} \tag{1}$$

where V_d and I_d are the average values of d-axis voltage and d-axis current, respectively. The approximation in (1) is valid since the d-axis current is closed-loop controlled at the value I_{Rs} by the FOC scheme. The value of stator resistance is then used to evaluate the average temperature of the stator winding as:

$$T_s(k) = \frac{R_s(k)}{R_{s,0}} \cdot \left(K_T + T_{s,0}\right) - K_T \tag{2}$$

where $R_{s,0}$ is the stator winding resistance evaluated at the starting of the heating procedure and so related to the initial winding temperature $T_{s,0}$, while K_T is the temperature coefficient of the conductive material (K_T = 234.5 for copper, K_T = 232.5 for aluminum).

2) Identification of the PM flux linkage

The evaluation of the PM flux linkage is performed through the PM-induced back-emf. Therefore, by imposing the zero-current condition through the FOC scheme, the (dq) voltages of the MUT coincide with the PM-induced back-emf. Besides, the variables of interest are computed as the average of all measurements performed in one mechanical revolution. In this way, the effects of the stator slots are compensated. Therefore, the PM flux linkage λ_m at the generic thermal point k (k = 1,…,n) is computed as:

$$\lambda_m(k) = \frac{V_q(k)}{p \cdot \omega_m(k)} \tag{3}$$

where V_q and ω_m are the average values of q-axis voltage and mechanical speed, respectively.

Finally, variables (1)-(3) are computed in the continuous-time domain as:

$$X(t) = X(k \cdot \Delta t) \qquad X = (R_s, T_s, \lambda_m) \tag{4}$$

III. PM Thermal Time Constant Computation

The experimental results that will be shown in Section IV demonstrate how the decay of the PM flux linkage can be described by a first-order model as:

$$\lambda_m(t) = \lambda_{m,\infty} + \left[\lambda_{m,0} - \lambda_{m,\infty}\right] \cdot e^{-\frac{t}{\tau_m}} \tag{5}$$

where τ_m is the PM's thermal time-constant while $\lambda_{m,0}$ and $\lambda_{m,\infty}$ are the values of the PM flux linkage at the starting and to the end of the test procedure, respectively. In detail, the second value is representative of the steady-state thermal condition of the MUT.

The PM's thermal time-constant τ_m is computed by using the method of the least squares on (5) and the experimental time-evolution (3), (4).

Although it is a significant approximation, the time-evolutions of both stator winding resistance and stator winding temperature can be described by a first-order model as:

$$\begin{cases} R_s(t) = R_{s,0} + \left[R_{s,\infty} - R_{s,0}\right] \cdot \left(1 - e^{-\frac{t}{\tau_s}}\right) \\ T_s(t) = T_{s,0} + \left[T_{s,\infty} - T_{s,0}\right] \cdot \left(1 - e^{-\frac{t}{\tau_s}}\right) \end{cases} \tag{6}$$

where $R_{s,\infty}$ is the stator winding resistance at the end of the heating procedure, corresponding to the steady-state thermal condition of the MUT windings $T_{s,\infty}$. Concerning τ_s, it can be considered as an equivalent thermal time-constant of the MUT. Therefore, such a time-constant is representative of the thermal path between the stator winding and the external environment.

The equivalent thermal time-constant τ_s is computed by using the method of the least squares on (6) and experimental time-evolutions (1), (2), (4).

IV. Experimental validation

The proposed measurement technique has been experimentally validated on three PMSMs. The first machine (MUT_1) is a spoke-rotor interior permanent magnet (IPM) motor having 8 poles. The second machine (MUT_2) is a fractional-slot surface-mount permanent magnet (SPM) motor having 36 poles. Finally, the third machine (MUT_3) is a SPM motor with distributed windings having 8 poles.

TABLE I. lists the main data of the MUTs.

A. Test Rig

The reference speed of the DM has been set at 300 r/m, 100 r/m, and 500 r/m for MUT_1, MUT_2, and MUT_3, respectively.

The mechanical rotor position has been measured with an incremental encoder having a resolution of 3600 pulses/rev.

The MUT converter has consisted of a three-phase VSI fed by a reversible dc source. The switching frequency has been set at 16 kHz.

The digital controller has consisted of the dSPACE® DS1103 while the sampling frequency has been set at 16 kHz, too (single-edge PWM).

TABLE I. PRIMARY DATA OF THE MACHINES UNDER TEST

-	MUT_1	MUT_2	MUT_3
Rotor type	IPM Spoke Rotor	SPM Outer Rotor	SPM Interior Rotor
Winding type	Concentrated	Concentrated	Distributed
Poles number	8	36	8
Rated power	600 W	800 W	1000 W
Rated speed	3000 r/m	166 r/m	3000 r/m
Rated voltage	190 Vrms	220 Vrms	28 Vrms
Rated current	2.75 Arms	5 Arms	30 Arms

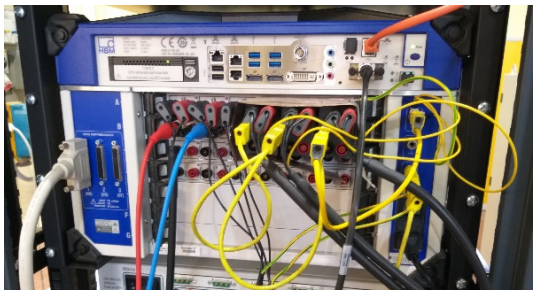

Fig. 5. View of the data recorder Gen7tA from HBM [24].

Finally, the data recorder has consisted of the Genesis 7tA (Gen7tA) from HBM [24], consisting of a high-performance transient recorder and data acquisition system, for measurements of line-to-line voltages, phase-currents, and the mechanical rotor position (Fig. 5). Thanks to its high-voltage/high-speed acquisition channels, the Gen7tA allows the direct measurement of the PWM line-to-line voltages. Besides, by using the software integrated with the instrument, the reconstruction of the time-fundamental voltage components can be performed.

B. Experimental results

In the following, experimental results obtained on the MUTs are presented, thus reporting the computed values of the thermal time-constants of PM τ_m and stator winding τ_s.

1) MUT_1

The decay of PM flux linkage and the increment of the stator winding temperature for the MUT_1 are shown in Fig. 6 and Fig. 7, respectively. Both PM and stator winding are in steady-state thermal conditions. The steady-state stator winding temperature is near to 132.6 °C, while the overall decline of PM flux linkage is about 24.7 %. Therefore, the PM of MUT_1 shows a strong temperature-dependent behavior. Finally, according to (5), (6), the computed values of thermal time-constants are τ_m = 36 min and τ_s = 48 min.

2) MUT_2

The decay of PM flux linkage and the increment of the stator winding temperature for the MUT_2 are shown in Fig. 8 and Fig. 9, respectively. The steady-state stator winding temperature is near to 100.7 °C, while the overall decline of PM flux linkage is about 5.9 %. Therefore, the PM of MUT_2 shows a robust temperature-independent behavior. Regarding the thermal time-constants, according to (5), (6), the computed values are τ_m = 44 min and τ_s = 32 min.

3) MUT_3

The PM of MUT_3 exhibits a temperature-independent behavior, thus obtaining experimental results similar to those of MUT_2, as shown in Fig. 10, and Fig. 11.

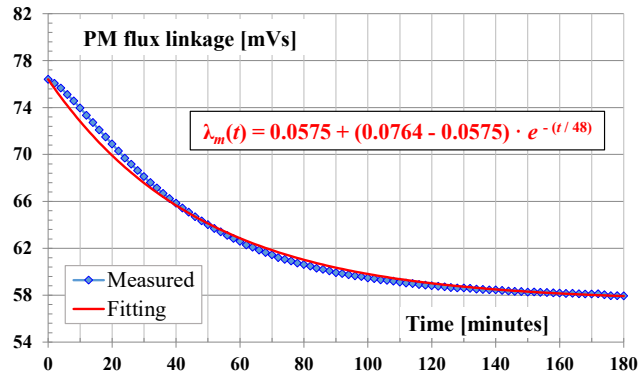

Fig. 6. Decay of the PM flux linkage for MUT_1.

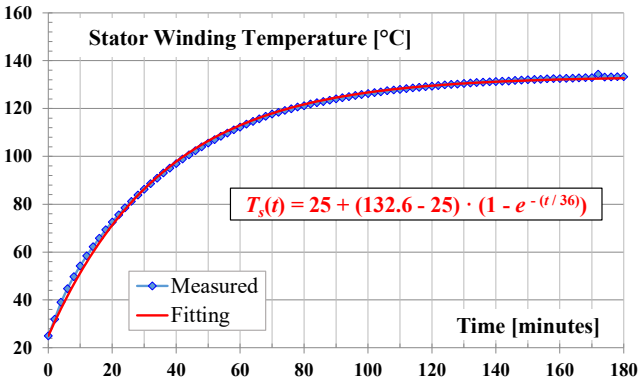

Fig. 7. Increment of the stator winding temperature for MUT_1.

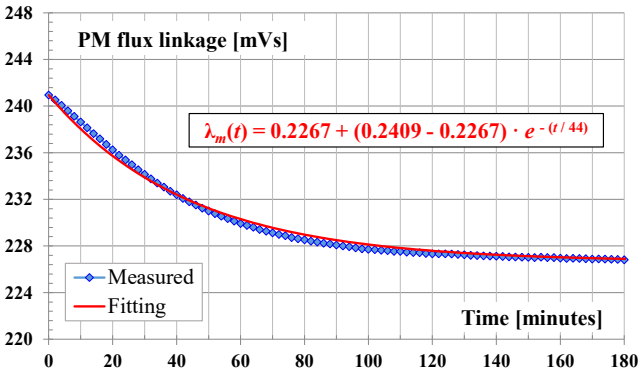

Fig. 8. Decay of the PM flux linkage for MUT_2.

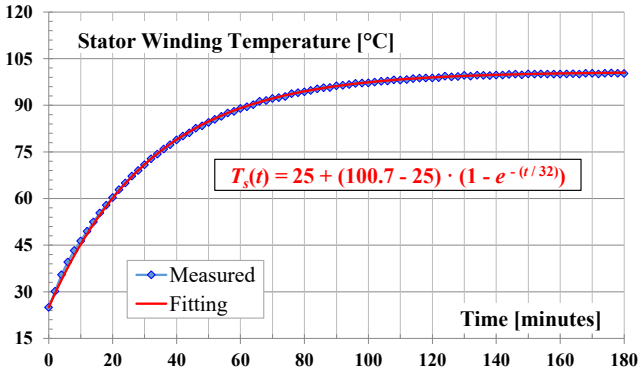

Fig. 9. Increment of the stator winding temperature for MUT_2.

The steady-state stator winding temperature is near to 69.5 °C, while the overall decline of PM flux linkage is about 3.9 %. In this case, the computed values of thermal time-constants for PM and stator winding are τ_m = 39 min and τ_s = 38 min, respectively.

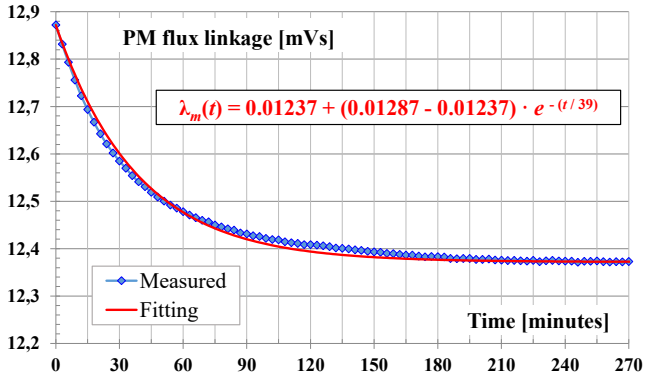

Fig. 10. Decay of the PM flux linkage for MUT_3.

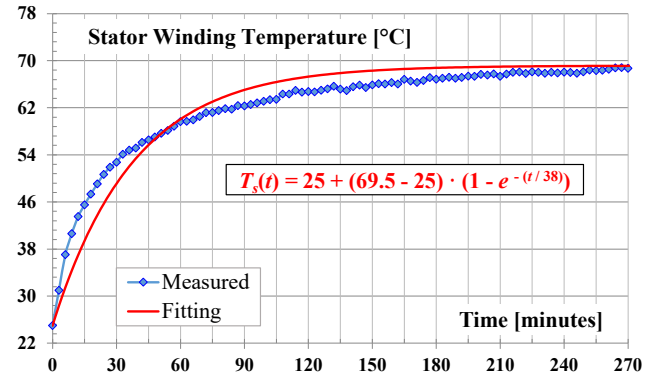

Fig. 11. Increment of the stator winding temperature for MUT_3.

TABLE II. SUMMARY OF THE OBTAINED EXPERIMENTAL RESULTS

-	MUT_1	MUT_2	MUT_3
$T_{s,0}$	25°C	25 °C	25°C
$T_{s,\infty}$	132.6 °C	100.7 °C	69.5 °C
τ_s	36 min	32 min	38 min
$\lambda_{m,0}$	76.4 mVs	240.9 mVs	128.7 mVs
$\lambda_{m,\infty}$	57.5 mVs	226.7 mVs	123.7 mVs
$R_{s,0}$	3.4 Ω	7.4 Ω	26 mΩ
τ_m	48 min	44 min	39 min

Finally, it is noted how for MUT_3, the use of a single time-constant to represents the time-evolution of the stator winding temperature is an approximation. Indeed, the time-constants that characterize the thermal path between the stator winding and the external environment are comparable from each other [8], [11], as also confirmed by the small time-duration of the thermal transient. Further considerations are not reported here since this paper is focused on the evaluation of the PM's thermal time-constant.

TABLE II. summarizes the results obtained for the three MUTs.

V. FINAL REMARKS

The time evolutions of the stator winding temperature and PM flux-linkage allow performing some assessments. The first one is related to the derating of the torque production caused by the decay of the PM flux linkage. Indeed, according to the FOC theory [21], the torque produced through the PM M_{PM} is computed as:

$$M_{PM} = \frac{3}{2} \cdot p \cdot \lambda_m \cdot i_q \tag{7}$$

Therefore, supposing that MUT is in steady-state thermal conditions and isothermal with the external environment (T_s=$T_{s,0}$), the injection of the rated MUT's current I_n (RMS) leads to the decay of the PM flux linkage as in (5). Although in the proposed test procedure, the injection of the rated current is performed along the *d*-axis, it is reasonable to think that in a real application such a current is distributed on both (*dq*) axes to maximize the torque production, leading to the maximum-torque per ampere (MTPA) operation of the drive. Since this paper is focused on the thermal behavior of the PM, it is supposed that the MUT current is injected only on the *q*-axis, thus maximizing the torque produced through the PM. Therefore, considering a continuative duty (S1) of the drive [25], the time evolution of the torque produced through the PM is:

$$M_{PM}(t) = M_{PM,\infty} + \left[M_{PM,0} - M_{PM,\infty} \right] \cdot e^{-\frac{t}{\tau_m}} \tag{8}$$

where the initial $M_{PM,0}$ and steady-state $M_{PM,\infty}$ torques are computed as:

$$\begin{aligned} M_{PM,0} &= \sqrt{2} \cdot \frac{3}{2} \cdot p \cdot \lambda_{m,0} \cdot I_n \\ M_{PM,\infty} &= \sqrt{2} \cdot \frac{3}{2} \cdot p \cdot \lambda_{m,\infty} \cdot I_n \end{aligned} \tag{9}$$

It is noted how the torque produced in steady-steady state thermal conditions depends on the decay of the PM flux linkage as:

$$k_M = \frac{M_{PM,\infty}}{M_{PM,0}} = \frac{\lambda_{m,\infty}}{\lambda_{m,0}} \tag{10}$$

where k_M stands for the derating factor of the torque production related to the PM heating. Therefore, thanks to the proposed test procedure, the evaluation of such a parameter can be performed, as demonstrated in (10). However, the derating of the MUT performance can also be evaluated in terms of efficiency. Indeed, considering that the MUT operates at the rated speed $\omega_{m,n}$, the mechanical power P_{out} is computed as:

$$P_{out}(t) = M_{PM}(t) \cdot \omega_{m,n} \tag{11}$$

Concerning the input power of the MUT P_{in}, by neglecting the iron losses, this is computed as:

$$P_{in}(t) = P_{out}(t) + P_J(t) \tag{12}$$

where according to (6), the Joule losses P_J are computed as:

$$P_J(t) = P_{J,0} + \left[P_{J,\infty} - P_{J,0} \right] \cdot \left(1 - e^{-\frac{t}{\tau_s}} \right) \tag{13}$$

It is noted how such losses depend on the initial and steady-state values of the stator resistance as:

$$\begin{aligned} P_{J,0} &= 3 \cdot R_{s,0} \cdot I_n^2 \\ P_{J,\infty} &= 3 \cdot R_{s,\infty} \cdot I_n^2 \end{aligned} \tag{14}$$

Finally, the MUT efficiency is computed as:

$$\eta(t) = \frac{P_{out}(t)}{P_{in}(t)} \tag{15}$$

In the following, the results of the above-presented analysis on the MUT_1 are shown.

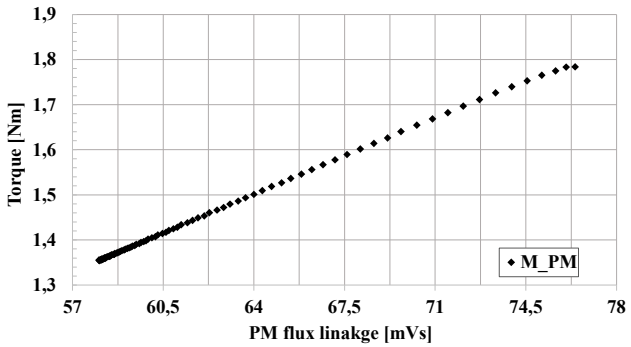

Fig. 12. Derating of the torque production for MUT_1.

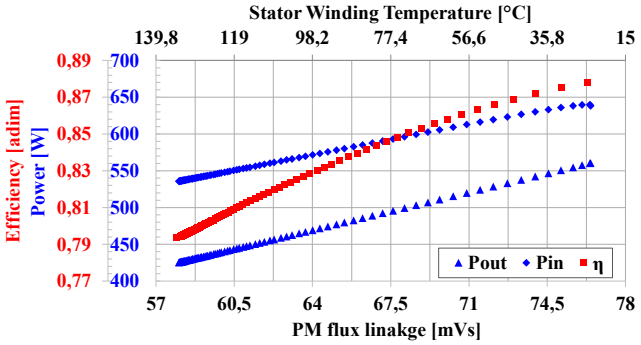

Fig. 13. Expected efficiency of the PM torque production for MUT_1.

According to the experimental results obtained on MUT_1 (Fig. 6 and Fig. 7), the decay of the PM flux linkage leads to a significant derating of the PM torque, as shown in Fig. 12. It is noted how, using (8), (10), the derating factor is near to $k_M = 0.752$, corresponding to a drop of the PM torque of about 24.7 %. Concerning the evolutions of the input and output MUT powers in rated operating conditions, together with the related efficiency, the expected results are shown in Fig. 13. It is noted how, supposing to inject the rated current of MUT to produce the PM torque, the increment of the stator winding temperature, and the simultaneous decay of the PM flux linkage, lead to a reduction of the MUT's efficiency near to 10 %. Indeed, the expected MUT's efficiency starts from a value of $\eta = 0.88$ up to reduce itself at a value near to $\eta = 0.79$ in steady-state thermal conditions.

VI. Conclusion

The paper proposes a new measurement technique for the identification of the permanent magnet (PM) thermal time-constant of synchronous ac motors. By injecting the rated current on the machine under test, the proposed test procedure performs the heating of both stator winding and PM.

In this way, thanks to a dedicated test rig that uses a data recorder, the time-evolutions of both stator windings temperature and PM flux linkage during the thermal transient can be evaluated. Based on the experimental results, the increment of the PM temperature can be described by a first-order model, so defining a single thermal time-constant.

Experimental results for three permanent magnet synchronous machines have been presented, demonstrating the validity of the proposed measurement technique. Finally, a preliminary analysis of the derating of machine performance due to the PM heating has been presented, thus demonstrating the effectiveness and utility of the proposed measurement technique.

References

[1] 'Ertrac - Welcome'. https://www.ertrac.org/ (accessed Mar. 19, 2020).

[2] Z. Q. Zhu and D. Howe, 'Electrical Machines and Drives for Electric, Hybrid, and Fuel Cell Vehicles', *Proc. IEEE*, vol. 95, no. 4, pp. 746–765, Apr. 2007.

[3] I. Boldea *et al.*, 'Automotive Electric Propulsion Systems With Reduced or No Permanent Magnets: An Overview', *IEEE Trans. Ind. Electron.*, vol. 61, no. 10, pp. 5696–5711, Oct. 2014.

[4] G. Pellegrino *et al.*, 'Comparison of Induction and PM Synchronous Motor Drives for EV Application Including Design Examples', *IEEE Trans. Ind. Appl.*, vol. 48, no. 6, pp. 2322–2332, Nov. 2012.

[5] T. Sebastian, 'Temperature effects on torque production and efficiency of PM motors using NdFeB magnets', *IEEE Trans. Ind. Appl.*, vol. 31, no. 2, pp. 353–357, Mar. 1995.

[6] S. Li, D. Han *et al.*, 'Analysis of the influence of temperature variation on performance of flux-switching permanent magnet machines for traction applications', in *2017 IEEE IEMDC*, May 2017, pp. 1–6.

[7] A. Boglietti *et al.*, and C. Mejuto, 'Evolution and Modern Approaches for Thermal Analysis of Electrical Machines', *IEEE Trans. Ind. Electron.*, vol. 56, no. 3, pp. 871–882, Mar. 2009.

[8] A. Boglietti, A. Cavagnino, and D. Staton, 'Determination of Critical Parameters in Electrical Machine Thermal Models', *IEEE Trans. Ind. Appl.*, vol. 44, no. 4, pp. 1150–1159, Jul. 2008.

[9] A. M. EL-Refaie, 'Fractional-Slot Concentrated-Windings Synchronous Permanent Magnet Machines: Opportunities and Challenges', *IEEE Trans. Ind. Electron.*, vol. 57, no. 1, pp. 107–121, Jan. 2010.

[10] A. Boglietti *et al.*, 'Winding Thermal Model for Short-Time Transient: Experimental Validation in Operative Conditions', *IEEE Trans. Ind. Appl.*, vol. 54, no. 2, pp. 1312–1319, Mar. 2018.

[11] A. Boglietti *et al.*, 'Stator-Winding Thermal Models for Short-Time Thermal Transients: Definition and Validation', *IEEE Trans. Ind. Electron.*, vol. 63, no. 5, pp. 2713–2721, May 2016.

[12] G. D. Demetriades *et al.*, 'A Real-Time Thermal Model of a Permanent-Magnet Synchronous Motor', *IEEE Trans. Power Electron.*, vol. 25, no. 2, pp. 463–474, Feb. 2010.

[13] C. Kral *et al.*, 'A Practical Thermal Model for the Estimation of Permanent Magnet and Stator Winding Temperatures', *IEEE Trans. Power Electron.*, vol. 29, no. 1, pp. 455–464, Jan. 2014.

[14] D. D. Reigosa *et al.*, 'Permanent-Magnet Temperature Distribution Estimation in Permanent-Magnet Synchronous Machines Using Back Electromotive Force Harmonics', *IEEE Trans. Ind. Appl.*, vol. 52, no. 4, pp. 3093–3103, Jul. 2016.

[15] M. Ganchev *et al.*, 'Sensorless rotor temperature estimation of permanent magnet synchronous motor', in *IECON*, Nov. 2011, pp. 2018–2023.

[16] M. Ganchev *et al.*, 'Compensation of speed dependency in sensorless rotor temperature estimation for permanent magnet synchronous motor', in *2012 ICEM*, Sep. 2012, pp. 1612–1618.

[17] E. Armando *et al.*, 'Measurement Technique for the Permanent Magnet Rotor Thermal Time Constant Determination', in *2020 ICIT*, Feb. 2020, pp. 193–198.

[18] E. Armando *et al.*, 'Experimental Identification of the Magnetic Model of Synchronous Machines', *IEEE Trans. Ind. Appl.*, vol. 49, no. 5, pp. 2116–2125, Sep. 2013.

[19] E. Armando, P. Guglielmi, G. Pellegrino, and R. Bojoi, 'Flux linkage maps identification of synchronous AC motors under controlled thermal conditions', in *2017 IEEE IEMDC*, May 2017, pp. 1–8.

[20] R. Bojoi *et al.*, 'Efficiency and loss mapping of AC motors using advanced testing tools', in *2016 ICEM*, Sep. 2016, pp. 1043–1049.

[21] P. Krause, O. Wasynczuk, S. D. Sudhoff, and S. Pekarek, *Analysis of Electric Machinery and Drive Systems*. John Wiley & Sons, 2013.

[22] G. Pellegrino *et al.*, 'Accurate Inverter Error Compensation and Related Self-Commissioning Scheme in Sensorless Induction Motor Drives', *IEEE Trans. Ind. Appl.*, vol. 46, no. 5, pp. 1970–1978, Sep. 2010.

[23] A. Boglietti, R. Bojoi, S. Rubino, and M. Cossale, 'Overload Capability of Multiphase Machines under Normal and Open-Phase Fault Conditions: a Thermal Analysis Approach', *IEEE Trans. Ind. Appl.*, vol. 56, no. 3, pp. 2560–2569, Mar. 2020.

[24] 'GEN7tA - High Channel Count Data Acquistion System and Tran', *HBM* (accessed Jun. 25, 2020).

[25] 'International Standard IEC 60034 - Rotating electrical machines'.